Experimental test of noncommutative quantum gravity by VIP-2 Lead

Kristian Piscicchia,[2,3] Andrea Addazi,[1,3,*] Antonino Marcianò,[4,3,†] Massimiliano Bazzi,[3] Michael Cargnelli,[5,3] Alberto Clozza,[3] Luca De Paolis,[3] Raffaele Del Grande,[6,3] Carlo Guaraldo,[3] Mihail Antoniu Iliescu,[3] Matthias Laubenstein,[7] Johann Marton,[5,3] Marco Miliucci,[3] Fabrizio Napolitano,[3] Alessio Porcelli,[5,3] Alessandro Scordo,[3] Diana Laura Sirghi,[3,8] Florin Sirghi,[3,8] Oton Vazquez Doce,[3] Johann Zmeskal,[5,3] and Catalina Curceanu[3]

[1]*Center for Theoretical Physics, College of Physics Science and Technology, Sichuan University, 610065 Chengdu, China*
[2]*Centro Ricerche Enrico Fermi—Museo Storico della Fisica Centro Studi e Ricerche "Enrico Fermi", 00184 Roma, Italy, EU*
[3]*Laboratori Nazionali di Frascati INFN, Frascati (Rome), 00044 Italy, EU*
[4]*Center for Field Theory and Particle Physics and Department of Physics Fudan University, 200438 Shanghai, China*
[5]*Stefan Meyer Institute for subatomic physics, Austrian Academy of Science, 1030 Vienna, Austria, EU*
[6]*Physik Department E62, Technische Universität München, 85748 Garching, Germany, EU*
[7]*Laboratori Nazionali del Gran Sasso INFN, 67100 Assergi (L'Aquila), Italy, EU*
[8]*IFIN-HH, Institutul National pentru Fizica si Inginerie Nucleara Horia Hulubei, 077125 Măgurele, Romania, EU*

(Received 25 March 2022; accepted 7 December 2022; published 4 January 2023)

Pauli exclusion principle (PEP) violations induced by space-time noncommutativity, a class of universality for several models of quantum gravity, are investigated by the VIP-2 Lead experiment at the Gran Sasso underground National Laboratory of INFN. The VIP-2 Lead experimental bound on the noncommutative space-time scale Λ excludes θ-Poincaré far above the Planck scale for non anishing "electriclike" components of $\theta_{\mu\nu}$, and up to 6.9×10^{-2} Planck scales if they are null. Therefore, this new bound represents the tightest one so far provided by atomic transitions tests. This result strongly motivates high sensitivity underground x-ray measurements as critical tests of quantum gravity and of the very microscopic space-time structure.

DOI: 10.1103/PhysRevD.107.026002

I. INTRODUCTION

The Pauli exclusion principle (PEP) is one of the main pillars of quantum mechanics, so deeply rooted in the foundations of physics to be the main responsible for the stability of atoms, nuclei, molecules, and matter in general. PEP forbids fermions to occupy the same quantum mechanical state, avoiding an arbitrary number of electrons or nucleons on the same orbital. It is worth reminding that PEP is a direct consequence of the spin-statistics theorem (SST), as proved by the same *W. Pauli* [1]: it arises from anticommutation rules of fermionic spinor fields, in the construction of the Fock space of the theory.

The SST is based on Lorentz invariance as a fundamental assumption. This means that the PEP is directly related to the fate of the space-time symmetry and structure. Nonetheless, Lorentz symmetry may be dynamically broken at a very high energy scale, without this phenomenon translating into a fundamental breakdown of the symmetry. In this case, the generation of nonrenormalizable operators, suppressed as inverse powers of the Lorentz violation scale Λ, is expected. On the other hand, approaches to quantum gravity, for which space-time coordinates *do non commute* close to the Planck scale (about 10^{19} GeV), thus deforming the Lorentz algebra at the very fundamental level, were put forward. The idea that the space-time might be noncommutative is usually accredited to *W. Heisenberg* (see, e.g., Ref. [2]), as an extension of the uncertainty principle, having been later elaborated by *H. Snyder* and *C.N. Yang* in Refs. [3,4]. From a symplectic-geometry approach [5], it is possible to unveil the deep relation intertwining space-time symmetries, statistics [6], and the uncertainty principle [7], hence providing concrete pathways for falsification.

Noncommutativity of space-time is common to several quantum gravity frameworks, to which we refer as noncommutative quantum gravity models (NCQG). The connection of space-time noncommutativity with both

*addazi@scu.edu.cn
†marciano@fudan.edu.cn

 © 2023 American Physical Society

string theory (ST) [8–12] and loop quantum gravity (LQG) [13–19] was extensively studied in literature.[1]

The two main classes of noncommutative space-time models embedding deformed Poincaré symmetries are characterized by κ-Poincaré [22–25] and θ-Poincaré [26–31] symmetries. Among these latter, there exists a subclass of models which preserves unitarity of the S matrix in the Standard Model sector [29,32]. From the experimental point of view, the most intriguing prediction of this class of noncommutative models is an energy dependent probability $[\delta^2(E)]$ for electrons to perform PEP violating atomic transitions. For both κ and θ Poincaré, the PEP violation probability turns to be of order one in the deformation parameter, when the probed energy is close to the scale of noncommutativity Λ (nonetheless, trivial dimensional arguments are sufficient to show that first order results in θ Poincaré are suppressed by the square of the energy scale). In the low energy regime, i.e., for energies much smaller than the noncommutativity scale, the PEP violation probability is highly suppressed, accounting for the lack of evidence of PEP violation signals over decades of experimental efforts in this direction.

The experimental tests of the spin-statistics connection are based on the search for signals of PEP violating processes, by exploiting different techniques, which may or not respect the Messiah and Greenberg (MG) [33] superselection rule. According to MG, even assuming small mixed symmetry components in a primarily antisymmetric wave function, in a system composed by a fixed number of particles the symmetry of the world Hamiltonian would prevent transitions among two different symmetry states, i.e., electrons or nucleons would not perform PEP forbidden transitions to lower orbits.

PEP tests for electrons, respecting the constraint imposed by MG, are performed by introducing new electrons in a preexisting system of electrons and constraining the probability that the newly formed state is symmetric. This was accomplished using various methods:

(i) the estimate of the primordial abundance of anomalous ^{5}Li, with three protons in the lowest level, leads to the limit ($\delta^2 < 2 \times 10^{-28}$) [34], which is also the strongest constraint inferred from astrophysical and cosmological arguments;

(ii) capture of ^{14}C β rays onto Pb atoms ($\delta^2 < 3 \times 10^{-2}$) [35];

(iii) pair production electrons captured on Ge ($\delta^2 < 1.4 \times 10^{-3}$) [36];

(iv) search for PEP violating atomic transitions in conducting targets, a prototype experiment of this class has been carried out in Ref. [37] following a suggestion of Greenberg and Mohapatra [38], it consists in measuring the x-ray emission from a target strip where a direct current is circulated and looking for a difference in the spectra acquired with current on and off (best upper limit $\delta^2 < 8.6 \times 10^{-31}$) [39,40];

(v) a generalized version of the latter experimental technique consists in using as test fermions the free electrons residing in the conduction band of the target, an improved version of the original analysis proposed in Ref. [36], based on the calculation of the time dependence of the anomalous x-ray emission process, lead to the best upper limit $\delta^2 < 1.53 \times 10^{-43}$ [41].

NCQG models are not subject to the MG superselection rule. Within this context, the prototype Reines-Sobel experiment [42] looked for anomalous transitions in a stable system, i.e., spontaneous PEP-violating transition in a closed system of electrons in an established symmetry state. In this framework strong bounds on the PEP violation probability were set by the DAMA/LIBRA Collaboration ($\delta^2 < 1.28 \times 10^{-47}$) [43], searching for K-shell PEP violating transitions in iodine—see also Refs. [44]. A similar strategy was followed by the MALBEK experiment [45], which set the bound $\delta^2 < 2.92 \times 10^{-47}$ by constraining the rate of K_α PEP violating transitions in germanium.

This research is based on a different strategy, which is not confined to the evaluation of a specific transition PEP violation probability. We consider the predicted PEP violating atomic transition amplitudes, in the context of the θ Poincaré model, whose derivation is outlined in Secs. III and IV. The deformation of the standard transition probabilities depends on the typical energy scales of the involved reactions, conditioned by the value of the "electric like" components of $\theta_{\mu\nu}$. This enables a fine tuning of the θ tensor components. The predicted energy dependence of the spectral shape of the whole complex of relevant transitions is accounted for and tested against the measured x-rays distribution, constraining Λ, for the first time, far above the Planck scale for $\theta_{0i} \neq 0$. Within a similar theoretical framework the DAMA/LIBRA limit on the PEP violating atomic transition probability [43] was analyzed in Ref. [31], and a lower limit on the noncommutativity scale Λ was inferred as strong as $\Lambda > 5 \times 10^{16}$ GeV, corresponding to $\Lambda > 4 \times 10^{-3}$ Planck scales.

PEP violating nuclear transitions were also investigated, e.g., in Refs. [43,46,47]. The strongest bound ($\delta^2 < 7.4 \times 10^{-60}$) was obtained in Ref. [46] searching for PEP violating transitions of nucleons from the $1P_{3/2}$ shell to the filled $1S_{3/2}$ shell. Based on a parametrization of the PEP-violation probability, in terms of inverse powers of the noncommutativity scale, the impact of these experimental results for

[1]The fact that noncommutativity emerges in both theories may not be a coincidence but can be conjectured to be instead related to a newly formulated **H**-duality—see, e.g., Refs. [20,21]—since a self-dual LQG formulation can be obtained from topological M theory. Besides ST and LQG contexts, deformed symmetries may effectively emerge from several other nonperturbative models of quantum geometry.

Planck scale deformed symmetries was investigated in Ref. [28]. As a result, a class of κ-Poincaré and θ-Poincaré models was excluded in the hadronic sector. Nonetheless, within the context of NCQG models, tests of PEP in the hadronic and leptonic sectors need to be considered as independent. There is no *a priori* argument why the standard model fields should propagate in the noncommutative space-time background with the same coupling. As an example, noncommutativity emerges in string theory as a by-product of the constant expectation value of the B-field components, which in turn are coupled to strings' world sheets with magnitudes that are not fixed *a priori*.

Underground x-ray surveys, searching for atomic transitions prohibited by the PEP, proved in recent years to provide very strong and promising tests of spin statistics [41,48,49] and, hence, tests of quantum gravity models at unexpectedly high noncommutativity scales. The results of the dedicated VIP-2 Lead experiment, searching for signals of K_α and K_β PEP violating transitions in an ultra radio-pure Roman lead target, are analyzed in the framework of NCQG, and summarized in Ref. [50]. We show that the experiment sets critical bounds on θ-Poincaré. In particular, VIP-2 Lead rules-out θ-Poincaré up to 2.6×10^2 Planck scales, if the "electric like" components of the $\theta_{\mu\nu}$ vector are non-null; θ-Poincaré is excluded up to 6.9×10^{-2} Planck scales if they vanish. VIP-2 Lead provides the strongest bound, from atomic levels transitions, on this special type of space-time noncommutativity.

II. THEORETICAL FRAMEWORK

At a formal level, the discussion on the fate of the spin-statistics theorem is strictly related to the deformation of the Poincaré symmetries, which is in turn induced by space-time noncommutativity. Few relevant caveats deserve to be represented with further detail than the one we deployed in the previous section, as these may affect the outputs of the theoretical investigation. We comment here that the arguments advocated in order to prevent the breakdown/deformation of the spin-statistics theorem, as a by-product of space-time noncommutativity, yield as a consequence that the theory can not be any longer falsifiable.

This issue has been tackled inspecting the validity of microcausality, within a quantum framework that is still required to be unitary. Intuitively, one expects the light cone not to retain any status in a noncommutative theory. It might then be surprising that in the case of the Moyal-plane noncommutativity, which we have referred to in the text as θ-Poincaré, for a certain class of observables, for instance, the one involving scalar fields with no time derivative, microcausality can still hold, namely,

$$[\mathcal{O}(x), \mathcal{O}(y)]_\star = [:\phi(x)\star\phi(x):, :\phi(y)\star\phi(y):]_\star = 0, \quad (1)$$

the equality being supposed to hold for spacelike separations, with $:\cdot:$ denoting a fixed ordering of the noncommutative coordinates, and the $\star$-product being defined by

$$:f(x)\star g(x) := \lim_{y\to x} f(x) e^{\frac{\iota}{2}\overleftarrow{\partial}^x_\mu \theta^{\mu\nu} \partial^y_\nu} g(y). \quad (2)$$

Problems related to a-causality for noncommutative theory were outlined in Ref. [51], in which the authors derived the commutator $[\mathcal{O}(x), \mathcal{O}(y)]_\star$. Similarly, using perturbation theory and different definitions of time ordering, it was pointed out in Ref. [52] that microcausality and unitarity cannot simultaneously coexist in noncommutative field theory. A similar result was obtained in Ref. [53], where it was found that SO(3,1) microcausality is violated, but that SO(1,1) microcausality in the light cone still holds when perturbative unitarity does. In Ref. [54], it was then pointed out that noncommutativity among space and time coordinates violates unitarity, unless lightlike noncommutativity is considered [55]. This problem was supposed to arise because of neglecting massive string states.

A different take on the same problem was developed in Ref. [56], where it was argued that for pure space noncommutativity micro-causality is preserved. As a by-product of this analysis, Pauli spin-statistics relation was shown in these cases to remain valid in noncommutative quantum field theories. Nonetheless, as pointed in Ref. [57], the special case inspected in Ref. [56] involves observables with no time derivatives. The implications of Ref. [56] for the spin-statistic theorem were then reframed in terms of the results found in [57], namely that the equal time commutator in D space-time dimensions,

$$[\mathcal{O}(x), \mathcal{O}(y)]_\star = (e^{-\iota p\cdot x - \iota p'\cdot y} + e^{-\iota p'\cdot x - \iota p\cdot y}) \frac{8\iota}{(2\pi)^{2D-1}} \int \frac{d^{D-1}k}{2E_k} \sin\left(-\frac{1}{2}\theta^{ij}(k_i(p+p')_j + p_i p'_j)\right) \times e^{\iota \vec{k}\cdot(\vec{x}-\vec{y})} \cos\left(\frac{1}{2}\theta^{ij}k_i p_j\right) \cos\left(\frac{1}{2}\theta^{ij}k_i p'_j\right), \quad (3)$$

does not vanish at spacelike separation. This latter result is instead consistent with previous ones derived in the literature—see, e.g., Refs. [51–55], and thus, hinges toward the confirmation that the spin-statistic theorem is violated.

The existence of eventual isomorphism has also been considered in order to instantiate a pure equivalence among commutative and noncommutative quantum field theories [58]—see also [59] for a critical insight. Notice that a

complete equivalence among the commutative and noncommutative theories, both at the level of the algebra and the coalgebra, would turn noncommutative theory to be unfalsifiable and unpredictive. Consequently, we do not deem as worthy of any phenomenological interest this theoretical approach, since it fails from distinguishing itself from the standard theory and its predictions, and thus decide not to speculate on the implications of this possibility.

III. TRANSITION AMPLITUDES

Noncommutative deformation as introduced by the $\star$-product induces deformation in standard processes of QED. The interaction vertex can be extracted from the action,

$$S = \int d^4x \left(-\frac{1}{4} F_{\mu\nu} \star F^{\mu\nu} + \bar{\psi} \star (\imath \not{D} \star - m) \psi(x) \right), \quad (4)$$

with covariant derivative expressed as $D_\mu^\star = \partial_\mu + \imath e A_\mu \star$, e denoting the electron charge, field strength of the electromagnetic field A_μ provided by $F_{\mu\nu} = \partial_\mu A_\nu - \partial_\nu A_\mu + \imath e [A_\mu{}^\star, A_\nu]$, with $[A_\mu{}^\star, A_\nu] \equiv A_\mu \star A_\nu - A_\nu \star A_\mu$ and fields undergoing the usual plane waves expansion,

$$\psi(x) = \sum_{s,k} [a^{(s)}(k) u^{(s)}(k) e^{-\imath k \cdot x} + b^{\dagger(s)}(k) v^{(s)}(k) e^{\imath k \cdot x}],$$
$$\bar{\psi}(x) = \sum_{s,k} [b^{(s)}(k) \bar{v}^{(s)}(k) e^{-\imath k \cdot x} + a^{\dagger(s)}(k) \bar{u}^{(s)}(k) e^{\imath k \cdot x}],$$
$$\not{A}(x) = \sum_{r,k} [\alpha^{(r)}(k) \not{\epsilon}^{(r)}(k) e^{-\imath k \cdot x} + \alpha^{\dagger(r)}(k) \not{\epsilon}^{(r)}(k) e^{\imath k \cdot x}],$$

with spinor indices $s = 1, 2$ labeling the set of four independent spinor solutions to the Dirac equation $\{u(k)^{(s)}, v(k)^{(s)}\}$, polarization indices $r = 1, 2$ labelling transverse traceless solution of the Maxwell equations $\epsilon_\mu^{(r)}$, and slash denoting contraction of vectors with $\gamma_m u$ matrices; summation is over discrete momenta $k = (k^{(0)}, \vec{k})$ in some regularization volume.

The $\star$-product induces deformed commutation and anticommutation rules,

$$a^{(s_1)}(p_1) a^{(s_2)}(p_2) = -e^{\imath p_1 \wedge_\theta p_2} a^{(s_2)}(p_2) a^{(s_1)}(p_1),$$
$$b^{(s_1)}(p_1) b^{(s_2)}(p_2) = -e^{\imath p_1 \wedge_\theta p_2} b^{(s_2)}(p_2) b^{(s_1)}(p_1),$$
$$\alpha^{(s_1)}(p_1) \alpha^{(s_2)}(p_2) = +e^{\imath p_1 \wedge_\theta p_2} \alpha^{(s_2)}(p_2) \alpha^{(s_1)}(p_1),$$

having introduced the antisymmetric product $a \wedge_\theta b \equiv a_\mu \theta^{\mu\nu} b_\nu$, and

$$a^{(s_1)}(p_1) a^{\dagger(s_2)}(p_2) = -e^{\imath p_1 \wedge_\theta p_2} a^{\dagger(s_2)}(p_2) a^{(s_1)}(p_1) + \delta_{\vec{p}_1, \vec{p}_2},$$
$$b^{(s_1)}(p_1) b^{\dagger(s_2)}(p_2) = -e^{\imath p_1 \wedge_\theta p_2} b^{\dagger(s_2)}(p_2) b^{(s_1)}(p_1) + \delta_{\vec{p}_1, \vec{p}_2},$$
$$\alpha^{(s_1)}(p_1) \alpha^{\dagger(s_2)}(p_2) = +e^{\imath p_1 \wedge_\theta p_2} \alpha^{\dagger(s_2)}(p_2) \alpha^{(s_1)}(p_1) + \delta_{\vec{p}_1, \vec{p}_2}.$$

Consistently with these rules, asymptotic in-coming and out-going two-fermion states are represented as

$$|p_1, s_1; p_2, s_2\rangle = a^{\dagger(s_1)}(p_1) a^{\dagger(s_2)}(p_2) |0\rangle = e^{\imath p_1 \wedge_\theta p_2} c^{\dagger(s_1)}(p_1) c^{\dagger(s_2)}(p_2) |0\rangle, \quad (5)$$

and

$$|p_1', s_1'; p_2', s_2'\rangle = a^{\dagger(s_1')}(p_1') a^{\dagger(s_2')}(p_2') |0\rangle = e^{\imath p_1' \wedge_\theta p_2'} c^{\dagger(s_1')}(p_1') c^{\dagger(s_2')}(p_2') |0\rangle, \quad (6)$$

having introduced ladder operators c and d phase shifted with respect to a and b by

$$a_{\vec{p}} = e^{-\frac{1}{2}\imath p \wedge_\theta P} c_{\vec{p}}, \qquad b_{\vec{p}} = e^{-\frac{1}{2}\imath p \wedge_\theta P} d_{\vec{p}}$$
$$\text{with} \quad P_\mu = \sum_{\vec{p}} (c_{\vec{p}}^\dagger c_{\vec{p}} + d_{\vec{p}}^\dagger d_{\vec{p}}),$$

and so forth for the Hermitian conjugates.

It is useful to consider the deformation of the Feynman amplitude $\mathcal{M}$ of the electron-muon scattering process, as recovered from the interaction vertex derived from Eq. (4) and from the asymptotic states in Eqs. (5) and (6). This reads

$$\mathcal{M}_\theta = e^{\frac{\imath}{2}(p_1 \wedge_\theta p_2 - p_1' \wedge_\theta p_2')} \mathcal{M}_0 e^{-\frac{\imath}{2}(p_1' \wedge_\theta p_1 + p_2' \wedge_\theta p_2)},$$
$$\mathcal{M}_0 = \frac{e^2}{2q^2} (\bar{u}^{s_1'}(p_1') \gamma^\mu u^{(s_1)}(p_1) \bar{v}^{s_2'}(p_2') \gamma_\mu v^{(s_2)}(p_2)),$$

with transferred momentum $q = p_1' - p_1 = p_2' - p_2$. Averaging over the initial spins and summing over final ones, the deformation rearranges, in the cross section σ, into a multiplicative factor,

$$\sigma_\theta = |\Phi_\theta|^2 \sigma_0,$$
$$\Phi_\theta = e^{\imath(p_1 \wedge_\theta p_2 - p_1' \wedge_\theta p_2')} e^{-\frac{\imath}{2}(p_1' \wedge_\theta p_1 - p_2' \wedge_\theta p_2)}.$$

The first order expansion in the θ tensor of $|\Phi_\theta|^2$ provides the PEP-violating phase $\phi_{\mathrm{PEPV}} = \delta^2$.

IV. ENERGY DEPENDENCE OF THE PEP VIOLATION PROBABILITY IN NCQG MODELS

Within the framework of NCQG models, the space-time noncommutativity is dual to a deformation of the Lorentz/Poincaré algebra and, hence, to new space-time symmetry algebras' structures (see, e.g., Refs. [60,61]). Specifically, in order to encode deformations of the Lie algebras of space-time symmetries, the concept of bialgebras, and the Hopf algebras, must be introduced. These two mathematical concepts, developed from an algebraic abstract viewpoint, have deep physical consequences, since the very same structure of the statistics of fermions and bosons is

there encoded. This property sets a direct connection between the microscopic structure of space-time, and the deformation of the spin-statistics relation, more specifically, the violation of PEP, which turns to be the observable for NCQG models. More in detail, the θ-Poincaré model leads to the prediction (see Refs. [28,62,63]) that PEP violations are induced with a suppression $\delta^2 = (E/\Lambda)^2$, where $E \equiv E(E_1, E_2, \ldots)$ is a combination of the characteristic energy scales of the transition processes under scrutiny (masses of the particles involved, their energies, the transitions energies, etc.).

For a generic NCQG model, deviations from the PEP in the commutation/anticommutation relations can be parametrized [28] as

$$a_i a_j^\dagger - q(E) a_j^\dagger a_i = \delta_{ij}. \tag{7}$$

For θ-Poincaré models,[2] when two electrons of momenta $p_i^\mu = (E_i, \vec{p}_i)$ (with $i = 1,\ 2$) are considered, we may introduce the phase ϕ_{PEPV} to parametrize the deformation of the standard transition probability W_0 into $W_\theta = W_0 \cdot \phi_{\mathrm{PEPV}}$. Making explicit Λ in the θ tensor through the relation $\theta_{\mu\nu} = \tilde{\theta}_{\mu\nu}/\Lambda^2$, with $\tilde{\theta}_{\mu\nu}$ dimensionless, the energy scale dependence may be introduced: (i) either according to

$$\phi_{\mathrm{PEPV}} = \delta^2 \simeq \frac{D}{2}\frac{E_N}{\Lambda}\frac{\Delta E}{\Lambda}, \tag{8}$$

where $D = p_1^0 \tilde{\theta}_{0j} p_2^j + p_2^0 \tilde{\theta}_{0j} p_1^j$, the quantity $E_N \simeq m_N \simeq A m_p$ denotes nuclear energy and $\Delta E = E_2 - E_1$ accounts for the atomic transition energy; (ii) or as an energy levels difference, encoding the PEP violating x-ray line energy, namely as in

$$\phi_{\mathrm{PEPV}} = \delta^2 \simeq \frac{C}{2}\frac{\bar{E}_1}{\Lambda}\frac{\bar{E}_2}{\Lambda}, \tag{9}$$

where $\bar{E}_{1,2}$ are the energy levels occupied by the initial and the final electrons and $C = p_1^i \tilde{\theta}_{ij} p_2^j$. The former case, discussed in Eq. (8), amounts to encode noncommutativity among space and time coordinates, namely $\theta_{0i} \neq 0$, while the latter case, in Eq. (9), corresponds to selecting $\theta_{0i} = 0$, which ensures unitarity of the θ-Poincaré models [53,54]. In both cases, the factors $D/2$ and $C/2$ can be approximated to unity.

We further notice that Eq. (7) resembles the quon algebra (see, e.g., Refs. [38,64]), in the case of quon fields; however, the q factor does not show any energy dependence, and it is not related to any quantum gravity model. Thus, the q model necessarily requires a hyperfine tuning of the q parameter. $q(E)$ is related to the PEP violation probability by

$$q(E) = -1 + 2\delta^2(E). \tag{10}$$

An experimental bound on the probability that PEP may be violated in atomic transition processes, straightforwardly translates into a constrain to the new physics scale Λ, consistently with the choice of the θ_{0i} components.

[2]In principle, there may exist other models, which may have an energy dependence from the electron momentum or mass. It is also interesting to remark that, in general, an angular dependence of the PEPV emission is expected.

V. THE VIP-2 LEAD EXPERIMENT

The VIP Collaboration is performing high precision tests of the Pauli exclusion principle (PEP) for electrons, in the extremely low cosmic background environment of the Gran Sasso underground National Laboratory (LNGS) of INFN. LNGS provides the ideal conditions for performing high-sensitivity searches of extremely low-rate physical processes. The overburden, corresponding to a minimum thickness of 3100 m w.e. (metres water equivalent), yields a reduction of the cosmic muon flux of about 6 orders of magnitude. As a consequence the main background source, apart from residual cosmic rays, is represented by the γ-radiation produced by long-lived γ-emitting primordial isotopes and their decay products, from the rocks of the Gran Sasso mountain and the concrete of the laboratory structure.

The VIP-2 Lead experimental apparatus is based on a high purity co-axial p-type germanium detector (HPGe), with a diameter of 8.0 cm and a length of 8.0 cm, surrounded by an inactive layer of lithium-doped germanium of 0.075 mm. The active germanium volume of the detector is 375 cm^3. The detector is surrounded by a complex of passive and active shieldings (the latter serves as target material). The passive shielding is composed of an outer pure lead layer (30 cm from the bottom and 25 cm from the sides) and an inner electrolytic copper layer (5 cm). The volume of the sample chamber is of about 15 l ($(250 \times 250 \times 240)$ mm^3). A 1 mm thick air-tight steel housing encloses the shielding structure and the cryostat and is flushed with boil-off nitrogen, from a liquid nitrogen storage tank, to minimize the radon contamination. With the aim to reduce the neutron flux impinging the detector this is also surrounded, on the bottom and the sides, by 5 cm thick borated polyethylene plates. The target consists of three cylindrical sections of radio-pure Roman lead, fully surrounding the detector. The thickness of the target is about 5 cm, for a total volume $V \sim 2.17 \times 10^3$ cm^3. The inner part of the setup is shown in Fig. 1 of Ref. [41]. A more detailed description of the external passive shielding and of the cryogenic and vacuum systems is given in Refs. [65,66]. The data acquisition system is a Lynx digital signal analyzer controlled via GENIE 2000 personal computer software, both from Canberra-Mirion.

TABLE I. Calculated PEP-violating K_α and K_β atomic transition energies in Pb (column labeled forb.). As a reference, the allowed transition energies are also quoted (allow.). Energies are in keV.

Transitions in Pb	allow. (keV)	forb. (keV)
$1s-2p_{3/2}$ $K_{\alpha 1}$	74.961	73.713
$1s-2p_{1/2}$ $K_{\alpha 2}$	72.798	71.652
$1s-3p_{3/2}$ $K_{\beta 1}$	84.939	83.856
$1s-4p_{1/2(3/2)}$ $K_{\beta 2}$	87.320	86.418
$1s-3p_{1/2}$ $K_{\beta 3}$	84.450	83.385

The aim of the measurement is to search for the x-rays signature of PEP-violating K_α and K_β transitions in Pb, when the $1s$ level is already occupied by two electrons. These transitions are shifted, with respect to the standard ones, as a consequence of the shielding effect of the additional electron in the ground state; hence, they are distinguishable in precision spectroscopic measurements. Let us notice that the deformation of the algebra preserves, at the first order, the standard atomic transition probabilities, the violating transition probabilities being dumped by factors $\delta^2(E)$; hence, transitions to the $1s$ level from levels higher then $4p$ will not be considered (see, e.g., Ref. [67] for a comparison of the atomic transitions intensities in Pb). The energies of the standard K_α and K_β transitions in Pb are given in Table I, where those expected for the corresponding PEP violating ones are also reported. The PEP violating K lines energies are obtained based on a multiconfiguration Dirac-Fock and general matrix elements numerical code [68]; see also Ref. [36], where the K_α lines are obtained with a similar technique.

The efficiency for the detection of x-rays emitted inside the Pb target, in the energy region of interest (defined in Sec. VI), was determined by means of Monte Carlo (MC) simulations. To this end, the detector was characterised and all of its components have been set into a MC code (Ref. [69]) based on the GEANT4 software library (Ref. [70]).

We present in Sec. VI, the results of a Bayesian analysis, aimed to extract the probability distribution function (*pdf*) of the expected number of photons emitted in PEP violating K_α and K_β transitions. The analyzed dataset corresponds to a total acquisition time $\Delta t \approx 6.1 \times 10^6$ s ≈ 70 d, i.e., about twice the statistics used in Ref. [41].

VI. DATA ANALYSIS AND RESULTS

The measured energy spectrum is shown in blue in Fig. 1, in the energy range $\Delta E = (65\text{–}90)$ keV. Considered the energy resolution of the detector in this region, which is $\sigma \simeq 0.5$ keV, the interval ΔE contains the K_α and K_β—standard and PEP violating—transitions in Pb. From a detailed analysis of the materials of the setup, these are the only emission lines expected in the selected range ΔE.

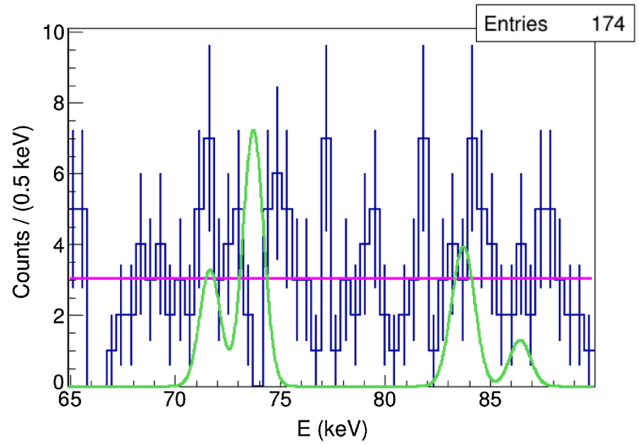

FIG. 1. The measured x-ray spectrum, in the region of the K_α and K_β standard and violating transitions in Pb, is shown in blue; the magenta line represents the fit of the background distribution. The green line corresponds to the shape of the expected signal distribution (with arbitrary normalization) for $\theta_{0i} \neq 0$.

However, due to the extreme radio purity of the target even the standard transitions of Pb cannot be recognized over the flat background, which corresponds to an average of about 3 counts/bin. We also notice that the target contributes to suppress the residual background eventually surviving the external passive shielding complex.

The aim of the analysis is to extract the upper limit $\bar{S}$ of the expected number of total signal counts, generated by PEP violating K_α and K_β transitions in the target. Comparison of $\bar{S}$ with the theoretically expected photons emission, due to PEP violating atomic transitions, provides a limit on the scale Λ of the model. The conditional *pdf* of the expected number of total signal counts S given the measured distribution—called *data*—is obtained as follows:

$$P(S|\text{data}) = \int_0^\infty \int_{\mathcal{D}_\mathbf{p}} P(S, B|\text{data}, \mathbf{p}) d^m\mathbf{p}\, dB, \quad (11)$$

where the joint posterior distribution of S and the expected number of total background counts B is given by the Bayes theorem,

$$P(S, B|\text{data}, \mathbf{p}) = \frac{P(\text{data}|S, B, \mathbf{p}) \cdot f(\mathbf{p}) \cdot P_0(S) \cdot P_0(B)}{\int P(\text{data}|S, B, \mathbf{p}) \cdot f(\mathbf{p}) \cdot P_0(S) \cdot P_0(B) d^m\mathbf{p}\, dS\, dB}. \quad (12)$$

In order to account for the uncertainties in the experimental parameters $\mathbf{p}$, which characterize the measurement and the data analysis, an average likelihood is considered, which is weighted with the joint *pdf* of $\mathbf{p}$. $\mathcal{D}_\mathbf{p}$ represents the domain of the parameters' space. The likelihood is parametrized as follows:

TABLE II. The table summarizes the resolutions ($\boldsymbol{\sigma}$) in keV, at the energies of the PEP violating K_α and K_β transitions.

Transitions in Pb	σ (keV)	Error (keV)
$K_{\alpha 1}$	0.492	0.037
$K_{\alpha 2}$	0.491	0.037
$1s-3p_{3/2}$ $K_{\beta 1}$	0.497	0.036
$1s-4p_{1/2(3/2)}$ $K_{\beta 2}$	0.498	0.036
$1s-3p_{1/2}$ $K_{\beta 3}$	0.497	0.036

$$P(\text{data}|S,B,\mathbf{p}) = \prod_{i=1}^{N} \frac{\lambda_i(S,B,\mathbf{p})^{n_i} \cdot e^{-\lambda_i(S,B,\mathbf{p})}}{n_i!}, \tag{13}$$

where n_i are the measured bin contents. The number of events in the ith bin fluctuates, according to a Poissonian distribution, around the mean value,

$$\lambda_i(S,B,\mathbf{p}) = B \cdot \int_{\Delta E_i} f_B(E,\boldsymbol{\alpha})\, dE + S \cdot \int_{\Delta E_i} f_S(E,\boldsymbol{\sigma})\, dE. \tag{14}$$

ΔE_i is the energy range corresponding to the ith bin; $f_B(E,\boldsymbol{\alpha})$ and $f_S(E,\boldsymbol{\sigma})$ represent the shapes of the background and signal distributions normalized to unity over ΔE. Among the experimental uncertainties the only ones which significantly affect $\bar{S}$ are those which characterize the shape of background (parametrized by the vector $\boldsymbol{\alpha}$) and the resolutions ($\boldsymbol{\sigma}$) at the energies of the violating transitions (the resolutions are reported in Table II). All the other experimental parameters are affected by relative uncertainties of the order of 1% (or less), which are neglected; hence, $\mathbf{p} = (\boldsymbol{\alpha},\boldsymbol{\sigma})$. For the normalized background shape, we take a flat distribution, as a result of the fit to the measured distribution described below. In order to obtain $f_S(E)$, the expected values of the numbers of PEP violating K transitions, predicted by the model, are to be evaluated.

A. Normalized signal shape

In order to describe the expected signal shape, corresponding to PEP violating electronic transitions, let us start noticing that electrons belonging to the $2s$ level are not allowed, at the first order in δ^2, to join the electrons belonging to $1s$. This is motivated by the fact that—at first order—the angular momentum selection rule is preserved by the deformation of the algebra.

We then consider the probability that one electron belonging to the $2p$ shell undergoes the violating $K_{\alpha 1}$ transition. This is conditioned to the fact that no other electron performs a transition to the $1s$; otherwise, the energy of the violating $K_{\alpha 1}$ transition would be shifted, as a result of the further shielding caused by the presence of three electrons in the ground state. The probability is then given by

$$\begin{aligned}
&\delta^2(E_{K_{\alpha 1}}) \cdot \Bigg[1 - 5 \cdot \delta^2(E_{K_{\alpha 1}}) \frac{BR_{K_{\alpha 1}}}{BR_{K_{\alpha 1}} + BR_{K_{\alpha 2}}} \\
&\quad - 5 \cdot \delta^2(E_{K_{\alpha 2}}) \frac{BR_{K_{\alpha 2}}}{BR_{K_{\alpha 1}} + BR_{K_{\alpha 2}}} \\
&\quad - 6 \cdot \delta^2(E_{K_{\beta 1}}) \frac{BR_{K_{\beta 1}}}{BR_{K_{\beta 1}} + BR_{K_{\beta 3}}} \\
&\quad - 6 \cdot \delta^2(E_{K_{\beta 3}}) \frac{BR_{K_{\beta 3}}}{BR_{K_{\beta 1}} + BR_{K_{\beta 3}}} - 6 \cdot \delta^2(E_{K_{\beta 2}}).\Bigg] \\
&= \delta^2(E_{K_{\alpha 1}}) \cdot [1 + C_{K_{\alpha 1}}].
\end{aligned} \tag{15}$$

In Eq. (15), the E_K represent the proper energy dependence to be considered in the PEP violation probability, function of the θ_{0i} choice [see Eqs. (8) and (9)]. The ratios among branching fractions are needed to weight the relative intensities of transitions which occur from levels with the same (n,l) quantum numbers, but different j (e.g., the $2p_{1/2}$ and the $2p_{3/2}$). Such distinction is necessary when the corresponding transition energies can be experimentally disentangled, since, for example, transitions as $4p \to 1s$ can not be resolved (the branching ratios are given in Table III). The term $C_{K_{\alpha 1}}$ introduces a second order correction in the searched violating transition probability (and hence, on Λ) which can be neglected. The rate of violating $K_{\alpha 1}$ transitions, predicted by the model, from the whole sample of Pb atoms in the target, which would be measured by the detector, is then given by

$$\Gamma_{K_{\alpha 1}} = \frac{\delta^2(E_{K_{\alpha 1}})}{\tau_{K_{\alpha 1}}} \cdot \frac{BR_{K_{\alpha 1}}}{BR_{K_{\alpha 1}} + BR_{K_{\alpha 2}}} \cdot 6 \cdot N_{\text{atom}} \cdot \epsilon(E_{K_{\alpha 1}}). \tag{16}$$

We mean with $\tau_{K_{\alpha 1}}$ the lifetime of the PEP-allowed $2p_{3/2} \to 1s$ transition (the lifetime for the generic transition will be indicated with τ_K, the lifetimes from Ref. [71] are summarized in Table IV; see also Ref. [42]). The $\epsilon(E_K)$ factors represent the detection efficiencies, for photons emitted inside the Pb target, at the corresponding violating transition energies E_K (the efficiencies are listed in Table III). The rate of the generic violating K transition Γ_K can be obtained by analogy with Eq. (16).

TABLE III. The table summarizes the values of the branching ratios of the considered atomic transitions and the detection efficiencies at the energies corresponding to the K_α and K_β forbidden transitions.

Forbidden transitions	BR	ϵ
$K_{\alpha 1}$	0.462 ± 0.009	$(5.39 \pm 0.11) \times 10^{-5}$
$K_{\alpha 2}$	0.277 ± 0.006	$(4.43^{+0.10}_{-0.09}) \times 10^{-5}$
$K_{\beta 1}$	0.1070 ± 0.0022	$(11.89 \pm 0.24) \times 10^{-5}$
$K_{\beta 2}$	0.0390 ± 0.0008	$(14.05^{+0.29}_{-0.28}) \times 10^{-5}$
$K_{\beta 3}$	0.0559 ± 0.0011	$(11.51^{+0.24}_{-0.23}) \times 10^{-5}$

TABLE IV. Values of the lifetimes of the PEP-allowed K transitions [71].

$\tau_{K_{\alpha 1}}$	1.64×10^{-17} s
$\tau_{K_{\alpha 2}}$	3.6×10^{-17} s
$\tau_{K_{\beta 1}}$	5.85×10^{-17} s
$\tau_{K_{\beta 2}}$	1.42×10^{-16} s
$\tau_{K_{\beta 3}}$	1.62×10^{-16} s

The probability to observe n violating $K_{\alpha 1}$ transitions in the time t is

$$P(n;t) = \frac{(\Gamma_{K_{\alpha 1}} t)^n e^{-\Gamma_{K_{\alpha 1}} t}}{n!}; \tag{17}$$

hence, the expected number of PEP violating $K_{\alpha 1}$ events, predicted by the model, which would be detected in the acquisition time Δt is

$$\mu_{K_{\alpha 1}} = \Gamma_{K_{\alpha 1}} \cdot \Delta t. \tag{18}$$

For a generic violating K transition, the expected number of events μ_K is given by analogy with Eq. (18).

Besides the *one step* violating K transitions, at the energies which are summarized in Table I, we should also consider two (or more) steps violating transitions populating the same lines. Namely events in which an electron from an atomic shell i undergoes a PEP violating transition to the np level ($n = 2, 3, 4$), followed by the violating K transition. The two steps process probability scales as $\delta^2(E_{i\to np}) \cdot \delta^2(E_{np\to 1s})$, thus introducing a second order correction to μ_K. The contribution of two (or more) steps violating transitions is then neglected.

Another set of processes to be accounted for consists in subsequent violating transitions from the same atomic shell np ($n = 2, 3, 4$) to $1s$. When an electron of the np undergoes a violating transition, it is replaced because of the (non-PEP violating) rearrangement of the atomic shells (the typical transition timescales being much smaller then the $\tau_K/\delta^2(E_K)$ lifetime of the violating process). As mentioned above, subsequent violating transitions would populate violating K lines, which are shifted in energy with respect to the transitions listed in Table I. The subsequent violating transition probability scales with the product of the δ^2, calculated at the energies corresponding to the two transitions; such processes (as well as higher order ones) are neglected in this analysis.

$f_S(E)$ is then given by the sum of Gaussian distributions, whose mean values (E_K) correspond to the energies of the PEP violating transitions in Pb, and the widths (σ_K) to the experimental resolutions at the energies E_K. The intensities of the violating lines are weighted by the rates Γ_K of the corresponding transitions [see Eq. (16)],

$$f_S(E) = \frac{1}{N} \cdot \sum_{K=1}^{N_K} \Gamma_K \frac{1}{\sqrt{2\pi\sigma_K^2}} \cdot e^{-\frac{(E-E_K)^2}{2\sigma_K^2}}. \tag{19}$$

It is worth noticing that the normalized signal shape depends on the choice of θ_{0i} (through the proper energy dependence term E_K which is contained in δ^2). Two independent analyses were then performed for the two θ_{0i} cases, by following the same procedure, in order to set constraints on the Λ scale of the corresponding specific model. f_S instead *does not* depend on Λ, since the dependence is re-absorbed by the normalization [see Eq. (20)]. In Eq. (19), the sum extends over the number N_K of PEP violating K transitions which are listed in Table I. The normalization is obtained by the condition,

$$\int_{\Delta E} f_S(E) dE = 1 \Rightarrow N = \sum_{K=1}^{N_K} \Gamma_K. \tag{20}$$

As an example, the shape of the expected signal distribution is shown (with arbitrary normalization) as a green line in Fig. 1 for the $\theta_{0i} \neq 0$ choice.

B. Normalized background shape

The normalized background shape is obtained from the best maximum log-likelihood fit to the measured spectrum, excluding $3\sigma_K$ intervals centered on the mean energies E_K of each violating transition. The best fit yields a flat background amounting to $L(E) = \alpha = (3.05 \pm 0.29)$ counts/(0.5 keV), the errors contain both statistical and systematic uncertainties. The normalized background shape is then

$$f_B(E) = \frac{L(E)}{\int_{\Delta E} L(E) dE}. \tag{21}$$

C. Prior distributions

For positive values of B, we choose a Gaussian prior distribution, with an expected value $B_0 = \langle B \rangle_G = \int_{\Delta E} L(E) dE$ and a standard deviation $\sigma_B = \sqrt{B_0}$. Zero probability is assigned to negative values of B. As a check, a Poissonian prior was tested for B; in this case, from the Bayes theorem, the expected value is $\langle B \rangle_P = B_0 + 1$ and $\sigma_B = \sqrt{\langle B \rangle_P}$. The upper limit on $\bar{S}$ is found not to be affected by this choice, within the experimental uncertainty.

For what concerns the choice of the prior $P_0(S)$, considered the *a priori* ignorance on the value of S, we opt for a uniform distribution in the range $(0 \div S_{\max})$, where $S_{\max}$ represents the maximum value of PEP violating x-ray counts in Pb, compatible with the best independent experimental bound (Ref. [36]) on the PEP violation probability. $S_{\max}$ is then obtained from Eq. (3) in Ref. [36], by substituting the number of free electrons in the conduction

TABLE V. Values of the parameters that characterize the Roman lead target, from left to right: free electron density, volume, mass, and number of free electrons in the conduction band.

n_e (m^{-3})	V (cm^3)	M (g)	N_{free}
1.33×10^{29}	2.17×10^3	22300	2.89×10^{26}

band of the target, the mean number of interactions and the efficiency with the corresponding parameters which characterize our experimental apparatus (see Tables III and V). We obtain $S_{max} \approx 1433$ and the prior on S is

$$P_0(S) = \begin{cases} \frac{1}{S_{max}} & 0 \le S \le S_{max} \\ 0 & \text{otherwise} \end{cases}. \tag{22}$$

D. Lower limits on the noncommutativity scale Λ

The joint pdf $P(S, B|\text{data})$ is shown in Fig. 2 for the case $\theta_{0i} \neq 0$. The upper limits $\bar{S}$ are calculated, for each choice of θ_{0i}, from the cumulative pdf ($\tilde{P}(\bar{S})$) by solving the integral equation,

$$\tilde{P}(\bar{S}) = \int_0^{\bar{S}} P(S|\text{data})\, dS = \Pi, \tag{23}$$

the values obtained for $\bar{S}$, corresponding to a probability $\Pi = 0.9$, are given in Table VI; they are affected by a relative numerical error of $\sim 2 \times 10^{-5}$.

A dedicated algorithm was developed for the calculation of the posterior pdf in Eq. (11) and of the cumulative distribution function. The numerical integrations are performed by means of Monte Carlo techniques and a detailed description of the numerical tools developed for this analysis is provided in the Appendix.

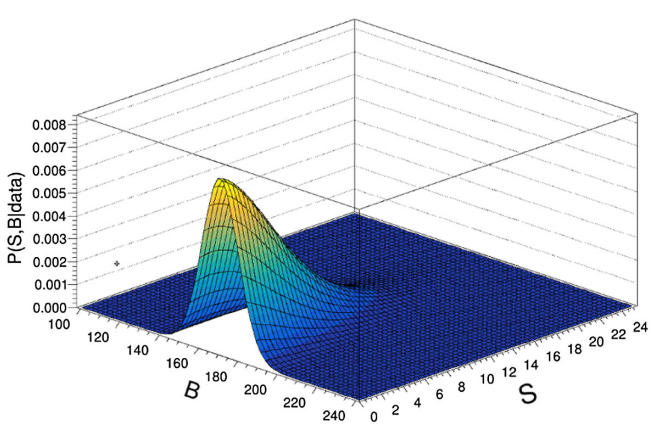

FIG. 2. Joint pdf $P(S, B|\text{data})$ of the expected number of total signal and background counts corresponding to $\theta_{0i} \neq 0$.

TABLE VI. The table summarizes the upper limits $\bar{S}$ on the expected numbers of signal counts, for a probability $\Pi = 0.9$, and the corresponding lower bounds on the noncommutativity scale Λ (in Planck scale unit), for the two choices of θ_{0i}.

θ_{0i}	$\bar{S}$	lower limit on Λ (Planck scales)
$\theta_{0i} = 0$	13.2990	6.9×10^{-2}
$\theta_{0i} \neq 0$	18.1515	2.6×10^2

The comparison of the total expected number of violating transitions μ predicted by the model and the corresponding upper bound $\bar{S}$, provides a constraint on the lower limit of the scale Λ, for each choice of θ_{0i},

$$\mu = \sum_{K=1}^{N_K} \mu_K = \frac{\aleph}{\Lambda^2} < \bar{S} \Rightarrow \tag{24}$$

$$\Rightarrow \Lambda > \left(\frac{\aleph}{\bar{S}}\right)^{1/2}. \tag{25}$$

The lower limits on Λ, corresponding to a probability $\Pi = 0.9$, are summarized in Table VI. This measurement rules out θ Poincaré if the "electriclike" components of $\theta_{\mu\nu}$ are taken different from zero, since in this case the scale Λ of noncommutativity emergence is constrained beyond the Planck scale. If, instead, $\theta_{0i} = 0$ the model is excluded up to 6.9×10^{-2} Planck scales.

VII. CONCLUSIONS

The results of the analysis of the data collected by the VIP-2 Lead experiment are presented. The measurement was devoted to the search for signals of Pauli exclusion principle violating K_α and K_β transitions, generated in a high radio-purity Roman lead target. A comparison is performed among the measured spectrum and the expected shape of the violating K-lines complex, as predicted in the framework of the θ-Poicaré noncommutative quantum gravity (NCQG) model, based on a Bayesian model. As a result θ Poicaré is excluded up to 2.6×10^2 Planck scales when the "electric like" components of the $\theta_{\mu\nu}$ tensor are different from zero, and up to 6.9×10^{-2} Planck scales if they vanish, thus providing the strongest atomic transitions based test of the model.

The most interesting phenomenological feature, emerging from the theory, consists on the PEP violating transition amplitude dependence on the characteristic energy scales involved in the investigated reactions [see, e.g., Eqs. (8) and (9)]. This, in turn, translates in a dependence on the atomic number of the adopted target, thus opening an intriguing scenario demanding a systematic analysis of the data from ongoing [43,45] and forthcoming experiments. Researches in analogy with what presented in

Refs. [28,31], addressed on a scan of possible evidences for spin-statistics violation, would supplement the conclusions of this study.

The VIP collaboration is presently implementing an upgraded experimental setup, based on cutting edge Ge detectors, aiming to probe θ Poincaré beyond the Planck scale, independently on the particular choice of the $\theta_{\mu\nu}$ electric like components. NCQG models, in a large number of their popular implementations, are not far to be tested and eventually ruled out. In this sense, contrary to naive expectations NCQG is not only a theoretical attractive mathematical idea but also offers a rich phenomenology, suitable to be tested in high sensitivity x-ray spectroscopic measurements.

ACKNOWLEDGMENTS

This publication was made possible through the support of Grant No. 62099 from the John Templeton Foundation. The opinions expressed in this publication are those of the authors and do not necessarily reflect the views of the John Templeton Foundation. We acknowledge support from the Foundational Questions Institute and Fetzer Franklin Fund, a donor advised fund of Silicon Valley Community Foundation (Grants No. FQXi-RFP-CPW-2008 and No. FQXi-MGB-2011), and from the H2020 FET TEQ (Grant No. 766900). We thank: the INFN Institute, for supporting the research presented in this article and, in particular, the Gran Sasso underground laboratory of INFN, INFN-LNGS, and its Director, Ezio Previtali, the LNGS staff, the Low Radioactivity laboratory for the experimental activities dedicated to the search of signals coming from the violation of the Pauli Exclusion Principle. We thank the Austrian Science Foundation (FWF) which supports the VIP2 project with the Grant No. P25529-N20, Projects No. P30635-N36, and No. W1252-N27 (doctoral college particles and interactions). K. P. acknowledges support from the Centro Ricerche Enrico Fermi—Museo Storico della Fisica e Centro Studi e Ricerche "Enrico Fermi" (Open Problems in Quantum Mechanics project). A. A. work is supported by the Talent Scientific Research Program of College of Physics, Sichuan University, Grant No. 1082204112427 and the Fostering Program in Disciplines Possessing Novel Features for Natural Science of Sichuan University, Grant No. 2020SCUNL209 and 1000 Talent program of Sichuan province 2021. A. M. wishes to acknowledge support by the Shanghai Municipality, through the Grant No. KBH1512299, by Fudan University, through the Grant No. JJH1512105, the Natural Science Foundation of China, through the Grant No. 11875113, and by the Department of Physics at Fudan University, through the Grant No. IDH1512092/001. A. A. and A. M. would like to thank Rita Bernabei and Pierluigi Belli for useful discussions on this subject.

APPENDIX: METHODS

1. Details of the integration algorithm

A dedicated algorithm was developed for solving the following integral equation:

$$\tilde{P}(\bar{S}) = \int_0^{\bar{S}} P(S|\text{data})\, dS = \int_0^{\bar{S}} \int_0^{\infty} \int_{\mathcal{D}_{\mathbf{p}}} P(S, B|\text{data}, \mathbf{p})\, d^m\mathbf{p}\, dB\, dS = \Pi. \quad \text{(A1)}$$

The integration over $d^m\mathbf{p}$ and dB is performed by using a Monte Carlo method, integration over dS is done by applying the trapezoidal rule. The range $[0, S_{\max}]$ is split in N_S intervals of width $h = S_{\max}/N_S$. This defines a vector $\{S_0, S_1, \ldots, S_{N_S}\}$ such that $S_i = i \cdot h$ with $i = \{0, 1, \ldots, N_S\}$. The posterior pdf of S is calculated for each value of S_i by solving the following integrals:

$$P(S_i|\text{data}) = \int_0^{\infty} \int_{\mathcal{D}_{\mathbf{p}}} P(S_i, B|\text{data}, \mathbf{p})\, d^m\mathbf{p}\, dB = \frac{P_0(S_i)}{\mathcal{N}} \int_0^{\infty} \int_{\mathcal{D}_{\mathbf{p}}} P(\text{data}|S_i, B, \mathbf{p}) \cdot f(\mathbf{p}) \cdot P_0(B)\, d^m\mathbf{p}\, dB, \quad \text{(A2)}$$

where $\mathcal{N}$ represents the normalization. The prior of S is defined as

$$P_0(S) = \frac{1}{S_{\max}} [\Theta(S) - \Theta(S - S_{\max})], \quad \text{(A3)}$$

where Θ is the Heaviside function. The prior of B is

$$P_0(B) = \frac{1}{\sqrt{2\pi B_0}} \exp\left(-\frac{(B - B_0)^2}{2B_0}\right) \cdot \Theta(B) = \mathcal{G}(B|\mathcal{N}_{B_0,B_0}) \cdot \Theta(B), \quad \text{(A4)}$$

with $B_0 \gg 0$.

The likelihood is weighted over a number $m = N_K + 2$ of experimental parameters $\mathbf{p} = (\boldsymbol{\alpha}, \boldsymbol{\sigma})$. The joint pdf of $\mathbf{p}$ is a multivariate Gaussian,

$$f(\mathbf{p}) = \mathcal{G}(\mathbf{p}|\mathcal{N}_{\mathbf{p}_0,\boldsymbol{\Sigma}}), \quad \text{(A5)}$$

whose mean values $\mathbf{p}_0 = (\boldsymbol{\alpha}_0, \boldsymbol{\sigma}_0)$ are defined by the fit parameters $\boldsymbol{\alpha}_0$ given in Sec. VI B and by the resolutions $\boldsymbol{\sigma}_0$ of the transition lines reported in Table II. The $m \times m$ covariance matrix is $\boldsymbol{\Sigma} = \text{diag}(\boldsymbol{\Sigma}_{\boldsymbol{\alpha}}, \boldsymbol{\Sigma}_{\boldsymbol{K}})$, with $\boldsymbol{\Sigma}_{\boldsymbol{\alpha}}$ and $\boldsymbol{\Sigma}_{\boldsymbol{K}}$ the corresponding uncertainties.

2. Monte Carlo integration

Equation (A2) can be rewritten as

$$P(S_i|\text{data}) = \frac{P_0(S_i)}{\mathcal{N}} \int_{-\infty}^{+\infty} \int_{\mathcal{D}_\mathbf{p}} P(\text{data}|S_i, B, \mathbf{p}) \cdot f(\mathbf{p}) \cdot \mathcal{G}(B|\mathcal{N}_{B_0,B_0}) \cdot \Theta(B) dB = \frac{P_0(S_i)}{\mathcal{N}} E_h[P(\text{data}|S_i, B)\Theta(B)],$$

where $h(B, \mathbf{p}) = \mathcal{G}(B|\mathcal{N}_{B_0,B_0}) \cdot f(\mathbf{p})$ is chosen as the importance sampling distribution and E_h represents the expectation value calculated over h. A set $\{(B_1, \mathbf{p}_1), \ldots, (B_{N_h}, \mathbf{p}_{N_h})\}$ of N_h values for the stochastic variables B and $\mathbf{p}$ are extracted according to the distribution $h(B, \mathbf{p})$. The $N_S + 1$ values of the posterior pdf of S are then estimated as follows:

$$P(S_i|\text{data}) = \frac{P_0(S_i)}{\mathcal{N}} \frac{1}{N_h} \sum_{j=1}^{N_h} P(\text{data}|S_i, B_j, \mathbf{p}_j)\Theta(B_j) = \frac{P_0(S_i)}{\mathcal{N}} \frac{1}{N_h} \sum_{j=1}^{N_h} \mathcal{I}(S_i, B_j, \mathbf{p}_j). \tag{A6}$$

3. Calculation of the cumulative $\tilde{P}(\bar{S})$

By applying the trapezoidal rule the normalization integral is approximated by

$$\mathcal{N} = \frac{1}{2N_S} \frac{1}{N_h} \sum_{i=1}^{N_S} \sum_{j=1}^{N_h} [\mathcal{I}(S_i, B_j, \mathbf{p}_j) + \mathcal{I}(S_{i-1}, B_j, \mathbf{p}_j)]. \tag{A7}$$

The ith value of the posterior is then obtained as

$$P(S_i|\text{data}) = \frac{\frac{2N_S}{S_{\max}} \sum_{j=1}^{N_h} \mathcal{I}(S_i, B_j, \mathbf{p}_j)}{\sum_{i=1}^{N_S} \sum_{j=1}^{N_h} [\mathcal{I}(S_i, B_j, \mathbf{p}_j) + \mathcal{I}(S_{i-1}, B_j, \mathbf{p}_j)]}, \tag{A8}$$

from which the cumulative distribution can be sampled as well; for a given $S = S_n$ with $n = \{0, 1, \ldots, N_S\}$, it is given by

$$\tilde{P}(S_n) = \frac{\sum_{i=1}^{n} \sum_{j=1}^{N_h} [\mathcal{I}(S_i, B_j, \mathbf{p}_j) + \mathcal{I}(S_{i-1}, B_j, \mathbf{p}_j)]}{\sum_{i=1}^{N_S} \sum_{j=1}^{N_h} [\mathcal{I}(S_i, B_j, \mathbf{p}_j) + \mathcal{I}(S_{i-1}, B_j, \mathbf{p}_j)]}. \tag{A9}$$

To conclude the value of $\bar{S}$ is obtained from a linear interpolation, among the two values S_k and S_{k+1} for which

$$\tilde{P}(S_k) < \Pi < \tilde{P}(S_{k+1}). \tag{A10}$$

[1] W. Pauli, Phys. Rev. **58**, 716 (1940).
[2] R. Jackiw, Nucl. Phys. B, Proc. Suppl. **108**, 30 (2002); *Letter of Heisenberg to Peierls (1930), Wolfgang Pauli, Scientific Correspondence*, edited by Karl von Meyenn (Springer-Verlag, Berlin, 1985), Vol. II, p. 15; Karl von Meyenn, *Letter of Pauli to Oppenheimer (1946), Wolfgang Pauli, Scientific Correspondence*, edited by Karl von Meyenn (Springer-Verlag, Berlin, 1993), Vol. III, p. 380.
[3] H. Snyder, Phys. Rev. **71**, 38 (1947).
[4] C. N. Yang, Phys. Rev. **72**, 874 (1947).
[5] C. Crnkovic and E. Witten, Report No. Print-86-1309 (PRINCETON); C. Crnkovic, Classical Quantum Gravity **5**, 1557 (1988); Nucl. Phys. **B288**, 419 (1987).
[6] M. Arzano and A. Marciano, Phys. Rev. D **75**, 081701 (2007).
[7] A. Addazi, P. Belli, R. Bernabei, A. Marcianò, and H. Shababi, Eur. Phys. J. C **80**, 795 (2020).
[8] J. Frohlich and K. Gawedzki, arXiv:hep-th/9310187.
[9] A. H. Chamseddine and J. Fröhlich, Some elements of Connes' noncommutative geometry, and space-time geometry, in *Yang Festschrift*, edited by C. S. Liu and S.-F. Yau (International Press, Boston, 1995), pp. 10–34 [arXiv:hep-th/9307012].
[10] J. Frohlich, O. Grandjean, and A. Recknagel, arXiv:hep-th/9706132.
[11] A. Connes, M. R. Douglas, and A. S. Schwarz, J. High Energy Phys. 02 (1998) 003.
[12] N. Seiberg and E. Witten, J. High Energy Phys. 09 (1999) 032.
[13] G. Amelino-Camelia, L. Smolin, and A. Starodubtsev, Classical Quantum Gravity **21**, 3095 (2004).
[14] L. Freidel and E. R. Livine, Phys. Rev. Lett. **96**, 221301 (2006).
[15] F. Cianfrani, J. Kowalski-Glikman, D. Pranzetti, and G. Rosati, Phys. Rev. D **94**, 084044 (2016).
[16] G. Amelino-Camelia, M. M. da Silva, M. Ronco, L. Cesarini, and O. M. Lecian, Phys. Rev. D **95**, 024028 (2017).
[17] G. Amelino-Camelia, M. M. da Silva, M. Ronco, L. Cesarini, and O. M. Lecian, Phys. Rev. D **95**, 024028 (2017).

[18] S. Brahma, M. Ronco, G. Amelino-Camelia, and A. Marciano, Phys. Rev. D **95**, 044005 (2017).
[19] S. Brahma, A. Marciano, and M. Ronco, arXiv:1707.05341.
[20] A. Addazi and A. Marciano, Sci. China Phys. Mech. Astron. **61**, 120421 (2018).
[21] A. Addazi and A. Marciano, Int. J. Geom. Methods Mod. Phys. **17**, 2050047 (2020).
[22] A. Agostini, G. Amelino-Camelia, M. Arzano, A. Marciano, and R. A. Tacchi, Mod. Phys. Lett. A **22**, 1779 (2007).
[23] M. Arzano and A. Marciano, Phys. Rev. D **76**, 125005 (2007).
[24] G. Amelino-Camelia, G. Gubitosi, A. Marciano, P. Martinetti, and F. Mercati, Phys. Lett. B **671**, 298 (2009).
[25] M. Arzano and J. Kowalski-Glikman, Phys. Lett. B **760**, 69 (2016).
[26] G. Amelino-Camelia, F. Briscese, G. Gubitosi, A. Marciano, P. Martinetti, and F. Mercati, Phys. Rev. D **78**, 025005 (2008).
[27] G. Amelino-Camelia, G. Gubitosi, A. Marciano, P. Martinetti, F. Mercati, D. Pranzetti, and R. A. Tacchi, Prog. Theor. Phys. Suppl. **171**, 65 (2007).
[28] A. Addazi, P. Belli, R. Bernabei, and A. Marciano, Chin. Phys. C **42**, 094001 (2018).
[29] A. Addazi and A. Marcianò, Int. J. Mod. Phys. A **35**, 2042003 (2020).
[30] A. Addazi and R. Bernabei, Mod. Phys. Lett. A **34**, 1950236 (2019).
[31] A. Addazi and R. Bernabei, Int. J. Mod. Phys. A **35**, 2042001 (2020).
[32] L. Alvarez-Gaume, J. L. F. Barbon, and R. Zwicky, J. High Energy Phys. 05 (2001) 057.
[33] A. Messiah and O. Greenberg, Phys. Rev. **136**, B248 (1964).
[34] M. H. Thoma and E. Nolte, Phys. Lett. B **291**, 484 (1992).
[35] M. Goldhaber and G. Scharff-Goldhaber, Phys. Rev. **73**, 1472 (1948).
[36] S. R. Elliott, B. H. LaRoque, V. M. Gehman, M. F. Kidd, and M. Chen, Found. Phys. **42**, 1015 (2012).
[37] E. Ramberg and G. A. Snow, Phys. Lett. B **238**, 438 (1990).
[38] O. W. Greenberg and R. N. Mohapatra, Phys. Rev. Lett. **59**, 2507 (1987).
[39] C. Curceanu *et al.*, Entropy **19**, 300 (2017).
[40] F. Napolitano *et al.*, Symmetry **14**, 893 (2022).
[41] K. Piscicchia, E. Milotti *et al.*, Eur. Phys. J. C **80**, 508 (2020).
[42] F. Reines and H. W. Sobel, Phys. Rev. Lett. **32**, 954 (1974).
[43] R. Bernabei, P. Belli, F. Cappella *et al.*, Eur. Phys. J. C **62**, 327 (2009).
[44] H. Ejiri *et al.*, Nucl. Phys. B, Proc. Suppl. **28A**, 219 (1992).
[45] N. Abgrall *et al.*, Eur. Phys. J. C **76**, 619 (2016).
[46] G. Bellini *et al.* (Borexino Collaboration), Phys. Rev. C **81**, 034317 (2010).
[47] Y. Suzuki *et al.* (Kamiokande Collaboration), Phys. Lett. B **311**, 357 (1993).
[48] H. Shi *et al.*, Eur. Phys. J. C **78**, 319 (2018).
[49] K. Piscicchia *et al.*, Entropy **22**, 1195 (2020).
[50] K. Piscicchia, A. Addazi, A. Marcianò *et al.*, Phys. Rev. Lett. **129**, 131301 (2022).
[51] N. Seiberg, L. Susskind, and N. Toumbas, J. High Energy Phys. 06 (2000) 044.
[52] H. Bozkaya, P. Fischer, H. Grosse, M. Pitschmann, V. Putz, M. Schweda, and R. Wulkenhaar, Eur. Phys. J. C **29**, 133 (2003).
[53] L. Alvarez-Gaume, J. L. F. Barbon, and R. Zwicky, J. High Energy Phys. 05 (2001) 057.
[54] J. Gomis and T. Mehen, Nucl. Phys. **B591**, 265 (2000).
[55] O. Aharony, J. Gomis, and T. Mehen, J. High Energy Phys. 09 (2000) 023.
[56] M. Chaichian, K. Nishijima, and A. Tureanu, Phys. Lett. B **568**, 146 (2003).
[57] O. W. Greenberg, Phys. Rev. D **73**, 045014 (2006).
[58] G. Fiore and J. Wess, Phys. Rev. D **75**, 105022 (2007).
[59] M. Chaichian, P. P. Kulish, A. Tureanu, R. B. Zhang, and X. Zhang, J. Math. Phys. **49**, 042302 (2008).
[60] S. Majid, Classical Quantum Gravity **5**, 1587 (1988).
[61] S. Majid and H. Ruegg, Phys. Lett. B **334**, 348 (1994).
[62] A. P. Balachandran, G. Mangano, A. Pinzul, and S. Vaidya, Int. J. Mod. Phys. A **21**, 3111 (2006).
[63] A. P. Balachandran, T. R. Govindarajan, G. Mangano, A. Pinzul, B. A. Qureshi, and S. Vaidya, Phys. Rev. D **75**, 045009 (2007).
[64] O. W. Greenberg, Phys. Rev. Lett. **64**, 705 (1990).
[65] H. Neder, G. Heusser, and M. Laubenstein, Appl. Radiat. Isot. **53**, 191 (2000).
[66] G. Heusser, M. Laubenstein, and H. Neder, Radioactive Waste Management and Environmental Restoration **8**, 495 (2006).
[67] M. O. Krause and J. H. Oliver, J. Phys. Chem. Ref. Data **8**, 329 (1979).
[68] P. Indelicato and J. P. Desclaux, MCDFGME, a multi-configuration Dirac-Fock and General Matrix Elements program (release 2005).
[69] M. Boswell *et al.*, IEEE Trans. Nucl. Sci. **58**, 1212 (2011).
[70] S. Agostinelli *et al.* (GEANT4 Collaboration), Nucl. Instrum. Methods Phys. Res., Sect. A **506**, 250 (2003).
[71] Payne, Wilbur Boswell, Relativistic Radiative Transitions (1955), LSU Historical Dissertations and Theses, 130, https://digitalcommons.lsu.edu/gradschool_disstheses/130.